Switching of a photochromic molecule on gold electrodes: single molecule measurements

Jin He[1], Fan Chen[1], Paul A Liddell[2], Joakim Andréasson,[2] Stephen D. Straight,[2] Devens Gust[2], Thomas A. Moore[2], Ana L. Moore[2], Jun Li[1], Otto F. Sankey[1] and Stuart M. Lindsay[1,2,3]

[1]Department of Physics and Astronomy, [2]Department of Chemistry and Biochemistry and [3]The Biodesign Institute, Arizona State University, Tempe, AZ 85287, USA

E-mail: Stuart.Lindsay@asu.edu; Gust@asu.edu

Abstract

We have studied the electronic changes caused by light-induced isomerization of a photochromic molecule between an open state (that absorbs in the UV to become closed) and a closed state (that absorbs in the visible to become open). Single molecule measurements of the molecular resistance show that it is 526±90 MΩ in the open form and 4±1 MΩ in the closed form when attached to gold break junction electrodes via thiol linkages. The corresponding ratio of open to closed resistance is in close agreement with the results of *ab initio* calculations, though the measured resistances are about half of the calculated values. Optical spectroscopy indicates that the switching isomerization occurs in both directions on small gold particles, evaporated thin gold films, and in the break junction experiments.

---

1. Introduction

The utility of molecules as electronic building blocks is generally judged by what we know of their solution properties, or in the case of electrochemical data their properties when in transient contact with a single electrode. Yet as devices shrink in size, and new functionalities are envisaged, the properties of the molecules when bonded to electrodes or sandwiched between electrodes become evermore important. The fundamental issue of how and why optoelectronic molecules function on metal surfaces at all has yet to be completely understood. It has long been known [1] that the lifetime of an excited state decays as $(z/\lambda)^{-3}$ at short distances, z, from a metal surface whereas charge transfer decays as $\exp -\beta z$ where β^{-1} is on the order of a few Angstroms or less. So strong is this excited state quenching effect that it overwhelms field-enhancement owing to a sharp metal probe near a chromophore, so that fluorescence is, in fact suppressed, not enhanced, near such a probe [2]. Yet optical function can be maintained on electrodes as evidenced by photoelectrochemical effects [3] and photoisomerization on an electrode [4]. Recently, Dulic *et al.* [5] showed that a photochromic molecule could be photoisomerized in one direction while it was being studied in a metal-molecule-metal junction. We have been engaged in a parallel study of a related photochromic molecule, using a new technique that allows us to characterize large numbers of molecules. We find both similarities and differences with this earlier study [5] and our results are described here. One outcome of this work is statistically well-characterized values for the resistance of the two isomers of the molecule.

Two photochromic dithienylethene molecules were investigated. One of these (**1**) bears a thiol group at each end (for bonding to gold), whereas the other (**2**) has only a

single thiol (Figure 1). Each molecule photoisomerizes from an open form (**1o** and **2o**, colorless in solution) to a closed form (**1c** and **2c**, deep blue in solution) on exposure to UV radiation. The reverse transition to the open form is driven by exposure to visible light. Thermal interconversion is very slow. We seek to determine the extent to which this transition between isomers takes place on the surface of a metal electrode and to measure the differences in the electrical conductivity of the two forms.

It has recently become possible to measure the conductivity of single molecules with some degree of precision. Pioneering work used break junctions [6, 7] or crossed wires [8, 9], but these are subject to some uncertainties: How many molecules are in the gap? What is the molecular geometry of their connections to the electrodes? Most of our data to date have been obtained with a self-assembled single molecule junction [10] because self-assembly defines the molecular geometries, and statistical analysis of the resultant data determines the number of molecules contacted. Importantly, measurements of molecular conductivity obtained with these methods gave results in reasonable agreement with first-principles calculations for the first time. However, the method is time consuming and cannot be applied to molecules that cannot be inserted into a self-assembled monolayer. In an alternative approach, Xu and Tao recently showed how a break junction, operated in a solution of dithiolated molecules, can be used to get statistically-significant data on single molecules [11]. Thousands of junctions are characterized at each value of bias applied, allowing statistical analysis of the data. To perform a measurement, a gold probe is pushed into a gold surface and pulled out again to form a thin gold filament. This will often break with a small number of molecules bonded to the gold at each end, and spanning the gap. Histograms of the current at a fixed

bias give a series of peaks corresponding to one, two, three etc. molecules in the junction. The junction structure cannot be characterized in the way that the self-assembled junctions can [10] but comparison of data obtained by both methods validates the choice of the smallest peak as the 'single molecule' datum [11, 12].

In this paper we report the results of measurements made with this new break-junction technique. We compare these with the results of first principles electronic structure calculations. We have also carried out spectroscopic studies of the photoisomerization of the molecules attached to metal surfaces and compared these with electronic measurements. Armed with our calibration of the conductivity of the two forms of the molecule we have tested the efficacy of nanofabricated junctions designed for embedding molecules in electronic circuits.

2. Materials and Methods

2.1. Synthesis

The synthetic route employed for preparation of dithiol **1** is shown in Figure 1. Palladium-catalysed Suzuki coupling of bromide [13] **3** with the known boronic acid [14] **4** in alkaline aqueous tetrahydrofuran gave the substituted aryl thiophene **5** in 68% yield. Lithiation of **5** with *n*-butyllithium followed by treatment with excess perfluorocyclopentene yielded the mono adduct **6**, in 89% yield. A second portion of **5** was lithiated, and **6** was added to give **7** in 59% yield. Hydrolysis of the protecting groups at 45º C in acidic tetrahydrofuran produced the dialdehyde **8**, which was subsequently reduced to the corresponding diol **9** with lithium aluminum hydride. Treatment of **9** using Mitsunobu conditions [15] in the presence of thioacetic acid gave

the dithioacetate **10** in 72% yield. The dithiol molecular switch **1** was prepared from **10** in 70% yield by treatment with acidic tetrahydrofuran. Monothiol **2** was prepared in a similar way. Structures were verified by ^{1}H-NMR spectroscopy, MALDI-TOF mass spectrometry, and UV-VIS spectrophotometry.

2.2. Break junction measurements

We use the method of Xu and Tao [11] in which a gold STM tip is repeatedly pushed into a gold surface in the presence of a solution of the dithiolated molecule (**1o** and **1c**) as shown schematically in Figure 2a. Data were acquired with a PicoSTM scanning probe microscope (Molecular Imaging, Phoenix). The current vs. time signal was recorded directly from the STM current amplifier output using a digital oscilloscope (Yokogawa DL 750). We used a hermetically sealed sample chamber flushed with argon to reduce oxygen and water vapor contamination. The STM tip was formed by cutting a 0.25 mm-diameter Au (99.999%) wire. The substrate was an Au (111) surface made by evaporation of 200 nm of Au onto a freshly cleaved heated mica substrate in ultra-high vacuum [16]. The substrates were re-annealed with a hydrogen flame immediately prior to use and rinsed with distilled toluene, then mounted on the microscope sample stage in a Teflon liquid cell, previously cleaned as described elsewhere [17]. Samples were submerged in freshly-distilled toluene and the sample chamber was kept flushed with Ar.

The surfaces were imaged by STM (Figure 3a) to check for cleanliness, and current vs. time data were recorded for this clean system (no molecules added). Typical traces are shown in Figure 3d where the time axis is converted to nm using the known z-

piezo sensitivity and the scanning voltage. The current vs. distance decays are rapid and structureless, a feature that disappears rapidly if the system becomes contaminated.

Solutions (0.2 μM) of the photochromic molecules in toluene, prepared in either the open or closed forms, were injected into the liquid cell and the surface was re-imaged. These molecules do not form ordered adlayers, but their adhesion to the surface is evident in the STM images as shown in Figures 3b (closed form injected) and 3c (open form injected). This change in surface texture is accompanied by the occurrence of plateaus in the current-distance recordings, as shown in Figures 3e and 3f.

2.3 Fixed nanojunctions

We used a number of approaches including self-terminating electrochemical etching/deposition [18] and electromigration [19] for generating fixed nanogaps on an oxidized Si surface. A schematic layout of such a device is shown in Figure 2b and an SEM image is shown in Figure 2c. Results were similar for all approaches and we confine our discussion here to gaps made with electromigration. The device fabrication starts with phosphorus doped *p*-type Si (100) wafer (ρ=0.002-0.02 Ω cm). The SiO_2 was thermally grown to a thickness of 200 nm on the Si substrate and an array of gold electrode pairs with a separation of 1.5μm was patterned on the surface by photolithography. Each gold electrode is 120 nm thick and 5 to 15 μm wide. In order to reduce leakage current when using electrochemical deposition and self-terminated electrochemical methods, we coated the electrodes with a 200 nm Si_3N_4 insulation layer by remote plasma-enhanced chemical vapor deposition (RPCVD) and opened 10 μm × 10 μm windows on the top of each gold electrode pair by reactive ion etching (RIE).

We used electron beam lithography (EBL) to make 60 nanometer wires that connected the larger electrodes. Devices were rinsed with acetone, ethanol and deionized water (18 MΩ) and cleaned with oxygen plasma or UV and ozone immediately prior to putting the chip in the vacuum chamber (10^{-7} Torr at room temperature), which was a part of a 4K probe station (Desert Cryogenics, Tucson, AZ). We used a semiconductor parameter analyzer (HP 4146B) to apply a voltage sweep to break the gold nanowires by electromigration [19]. The nanowires had resistances of about 100 Ω before being broken, increasing to values between MΩ and GΩ on breaking. The device arrays were then removed from the vacuum system and immediately submerged in solutions of the molecules in toluene (typically 0.2 μM) overnight. After rinsing with freshly distilled solvent and drying in clean argon, the arrays were returned to the vacuum station for electrical characterization. Here, we report results for junctions in which resistance fell after exposure to the solution of molecules, indicating the possible attachment of one or more molecules across the gap.

2.4. Optical spectroscopy

Optical spectroscopy of molecules on metal surfaces has been carried out previously using gold nanoparticles suspended in a solvent [5, 20], but this leaves open the possibility that molecules could leave the surface, photoisomerize, and become reattached. We therefore made optically transparent thin films of gold so that the spectroscopy could be carried out in a gaseous atmosphere. Au (nominal thickness 1 nm) was sputtered onto a freshly-cleaved mica surface, producing islands of 50 to 100 nm diameter that are electrically unconnected on the gold surface (as deduced from AFM

studies). Though this substrate was transparent, its optical absorption spectrum was similar to that of bulk gold (see below, and note the recent report of an alternative [21]). These surfaces were soaked for 10 min in a solution of dithienylethene **1** or **2** in 2-methyltetrahydrofuran, rinsed thoroughly, and allowed to dry.

For the UV-induced closing reaction, a UVP UV lamp (Model UVGL-25, 366 nm 1.5 mW/cm^2) was used. For the opening reaction, the light was produced by a Xe/HgXe-lamp (ORIEL Corp. Model 66028). Before the slides were illuminated with the Xe-lamp, the IR portion of the light was reduced by passing the beam through two water-cooled IR filters (A = 5 and A = 9 at 900 and 1060 nm, respectively). In addition, a long wavelength pass filter was used to remove wavelengths shorter than 590 nm. The resulting light power density on the slides was 40 mW/cm^2. During the measurements, the slides were kept under an argon atmosphere in a 10 × 10 mm absorption cell.

3. Results and theoretical modeling

3.1. Single molecule conductivity measurements

Histograms of the current measured at a series of fixed biases are shown for the dithiol-bearing molecules in the open form **1o** (Figure 4a) and the closed form **1c** (Figure 4b). When the molecules are in solution in organic solvents, visible light drives the population essentially entirely into the open form, but some UV absorption by the closed form results in an equilibrium photostationary state population on exposure to UV illumination. In deuteriochloroform solution, **1** reaches a photostationary state containing 80% **1c** and 20% **1o** under 366 nm illumination, as described in section 2.4. Thus, there are some small-current data points in the nominally closed population, but the range of

the histogram has been chosen so as to show only data for the closed form (the population of the two forms on the electrode surface is discussed below). Note the characteristic peaks at integer multiples of a lowest conductance (the lowest peak). Following Xu and Tao [11], we identify this first peak with the smallest current step, corresponding to one molecule spanning the gap. The peaks were fitted with Gaussians (outlines shown in white on the Figure) to determine the current corresponding to each maximum. The results are tabulated in Table 1, which shows how the ratios of the currents corresponding to successive peaks are approximately integer multiples. The corresponding current vs. voltage data are summarized in Figure 5 for (a) the open molecules and (b) the closed molecules. Most data were taken in only one bias direction and the data folded around zero bias. This procedure was checked by recording data at one bias with the bias reversed. This was done because although the molecules themselves are symmetric, their spatial arrangement in the gaps is unknown, and the initial structure of the junctions is asymmetric (sharp probe vs. flat surface). This test indicated that the data were symmetric about zero bias. This symmetry of the I-V curves implies that the junction as pulled is symmetric, probably a result of the pulling out of gold filaments from each electrode [22]. Error bars correspond to the half widths of the Gaussian fits (the absolute error on the fitting parameters was too small to show on this scale). Linear fits to these measurements show that the resistance is 526±90 MΩ in open form **1o** and 4±1 MΩ in the closed form **1c**. Note that the voltage range over which data could be obtained in the open form (±0.2 V) was larger than the corresponding range in the closed form (±0.12 V). This limit was set by the onset of increasing noise (see below).

3.2. Theoretical Modeling

Calculations of the theoretical current-voltage curve for the photochromic molecule were based on the Landauer-Buttiker formalism [23, 24] with the transmission function calculated using quantum mechanical scattering theory [25, 26]. The model system was an infinite 2-d lattice (monolayer) of dithienylethene molecules sandwiched between gold contacts made up of eight ideal (3 × 3) Au (111) layers in a supercell structure as discussed in detail elsewhere [27]. The self-consistent Kohn-Sham single electron states were obtained for this system using Fireballs[28-30], a local atomic-orbital density-functional theory (DFT) based method in the pseudopotential local-density approximation (LDA). The present procedures have been previously found to give good agreement with experiments on other organic molecules [31]. The Green's functions needed to compute the current-vs.-voltage curves were calculated from the Hamiltonian and overlap matrix elements. Though the electronic structure calculation is performed with gold slabs of finite thickness, we extend the Green's functions to include semi-infinite contacts using a block-recursion technique. Full details and related descriptions are given elsewhere [12, 27].

The current is calculated as

$$I(V) = \frac{2e^2}{h} \int T(E,V)\left[f(E - eV/2) - f(E + eV/2)\right] \qquad (1)$$

where $T(E,V)$ is the transmission function [25, 26], f is the Fermi function, and V is the voltage. We have assumed that the electron energies in the electrodes are shifted symmetrically by $+eV/2$ and $-eV/2$ for the left and right electrodes, respectively. The calculations of the metal-molecule-metal ensemble are fully self-consistent at zero bias, and thus include charge transfer effects at the interface; however, the effects of bias and

the electric field are approximated by shifts in the Fermi levels of the left and right contacts.

The electronic current is determined using an optimized molecular structure obtained from Hartree-Fock theory, but the electronic structure of the dithienylethene-gold system [32, 33] is obtained from DFT. The details of the contact between the molecule and metal are important. We consider two typical molecule-metal contact sites, on-top and hollow sites, to allow for our uncertainty about the interface between dithienylethenes and the gold surface. The distance between sulfur and these two contact sites, on-top [34] and hollow [35], is 2.42 Å and 1.9 Å, respectively. Although thiolated molecules generally are energetically preferred within DFT to reside at the hollow site, the experimental pulling technique used in this work may result in a contact closer to the on-top bonding.

Besides the contact geometry, there are uncertainties concerning angles of orientation of the molecule in relation to the surface. We chose configurations so that the molecule is symmetrically bonded between two parallel gold slabs with the surface (vertical)-S-C angle close to 110^0. Based on these considerations, I-V curves were therefore computed for arrangements in which the molecule was rotated about the surface normal on a fixed conical surface [36]; these rotations produce a "shadow" of the molecule along different directions of the gold surface. The I-V characteristics were calculated for contacts at the two bonding sites (on-top and hollow), and each curve was averaged from the results for 4 rotation angles about the normal.

Calculated I-V curves for the two cases (hollow site and on-top site) are shown for the open form of the molecule in Figure 5a and the closed form in Figure 5b.

Calculated currents are about 2 times smaller than the measurements, with the best agreement occurring for the on-top site. The theoretical ratio of the closed to open resistances is 177 for the on-top site, and 91 for the hollow site; these are in accord with the experimentally determined value of 131.

3.3. Spectroscopic study of switching on gold surfaces

Figure 6 shows results of absorption measurements of dithiolated dithienylethene molecule **1** as a self-assembled monolayer on a 1 nm gold film deposited on mica, as discussed in Section 2.4. The molecule was applied in the open (colorless) form **1o**. Absorption spectra were taken under an argon atmosphere in the absence of solvent. The spectra shown are difference spectra, wherein the spectrum initially obtained of the open form on the gold slide has been subtracted. This removes much of the gold plasmon absorption and scatter. Hence, the spectra show only the *change* in absorption after light exposure. Figure 6a shows the results of irradiation using UV light. The band at ~650 nm grows in with irradiation time, and is assigned to the closed, colored form of the molecule **1c**. (This is verified by the similarity of this band to that obtained from the closed form in solution, or on the gold surface.) In Figure 6b, the same slide, with the molecule now mainly converted to the closed form, is irradiated with red (>590 nm) light. The amplitude at 650 nm decreases with irradiation time, signaling isomerization of the closed form back to the open, colorless structure. Thus, isomerization occurs in both directions on the gold surface. The dotted curve in Figure 6a was obtained by taking the sample after 21 min of UV irradiation followed by 290 min of irradiation with red light (lowest curve at 650 nm in Figure 6b) and irradiating once again with UV light for 20

min. Closing of the molecule is again observed, proving that the results in the Figure are due to photoisomerization while the molecule is attached to gold, rather than to decomposition. These studies were repeated for the monothiolated molecule **2** (data not shown) with similar results, although the opening time under the irradiation conditions employed was somewhat faster for **2c** (123 min) than for **1c** (506 min).

3.4. Conductance switching in-situ

In this series of experiments, we investigated the photoisomerization reactions of **1** on a gold surface as detected by single molecule conductance. The dithiolated molecules, prepared initially in either the open or closed state, were adsorbed onto the gold substrate by exposing it to a 0.2 μM toluene solution for 40 min. The surface was thoroughly rinsed with toluene to remove molecules not bonded to the surface and then submerged in toluene for the initial conductance measurements. The substrate was then exposed to the appropriate switching radiation, and the conductance measured again. In the case of molecules that were applied in the open state (**1o**) this radiation was UV at 366 nm (from a UVP, UVGL-25 lamp) with an illumination intensity of approximately 1.5 mW/cm^2 for 15 min (shorter wavelengths resulted in photodegradation of the molecules). In the case of the molecules that were applied in the closed state, the sample was exposed to an expanded 647 nm beam from an Ar/Kr laser (Melles Griot, 643 AP tunable ion laser) at an intensity of 2.1 mW/cm^2 for 15 min.

In all of these experiments, conductance data were obtained in both the ranges expected for open and for closed molecules. The relative fraction of measured molecules in each state after illumination are shown by the bar graphs in Figure 7 (error bars are ±1

sd). For the experiments shown in Figure 7a, the study began with a sample to which a solution of **1** mostly in the closed state **1c** (as determined from UV-VIS spectroscopic measurements) was applied. About 70% of the molecules giving a response in the break junction were found to be closed (Figure 7a, first set of bars). Subsequent exposure to 647 nm radiation as described above resulted in approximately equal populations of the open and closed isomers (second set of bars). Thus, photoinduced opening occurs on the surface. Note that the amount of visible irradiation used was much less than that employed in the optical experiments discussed above. Finally, exposure to 366 nm radiation resulted in an increase in the fraction of closed molecules (Figure 7a, third set of bars). These data show that both light-induced opening of **1c** and light-induced closing of **1o** occur on the gold substrate used in the nanojunction apparatus.

The complementary experiment shown in Figure 7b began with the photochromic molecules bonded to the substrate mostly in the open state (67±5% **1o**, 33±4% **1c**, first set of bars in the Figure). After irradiation under toluene at 366 nm as discussed above for 20 min, the conductance measurements yielded the data in Figure 7b, second set of bars; 59±3% of the molecules measured were the **1o** isomer, and 41±3% were the closed form **1c**.

Figure 7 demonstrates that the photochrome isomerizations occur on the gold surface used for the break junction measurements, as well as in solution and on the thin gold films. However, the apparent efficiency of the UV-induced photoisomerization to form **1c** (as determined by the break junction results) is reduced when the molecules are attached to the metal surface used in the nanojunction apparatus.

3.5 Measurements in fixed gaps

Armed with reasonably accurate measurements of the resistance of the dithiolated dithienylethene molecules **1** in both the open and closed states, we sought to test the frequency with which the 'correct' value of single molecule resistance could be recorded when the molecules were inserted into nanofabricated fixed gaps. It is well known that insertion of molecules into fixed nanogaps yields a wide variety of values for the final resistance, so that 'good' gaps have to be selected. Thus a characterization of the distribution from which this selection is made is important. Additional concerns stem from the observation of complex electrical characteristics in junctions made by electromigration into which no molecules have been inserted deliberately [37].

We selected gaps that showed evidence of a clear drop in resistance after insertion of molecules (see methods above) and measured their resistance at low bias. In the case of the closed molecules **1c**, we found a total of 29 such gaps, while in the case of the open molecules, we found 85 gaps.

The measured resistances were distributed over a wide range of values. In order to display the results, we counted the number of gaps measured in each decade of resistance values, and then plotted this as a fraction of the total number of gaps on a logarithmic resistance scale. The results are shown in Figure 8. Approximately 15% of the gaps gave values in the 'right' range. However, the overall distribution of resistances does not correlate at all with the isomeric state of the inserted molecules: the distributions actually skew in a direction opposite to that expected. In other words, there were more measured values at high resistance in the case of the closed (low resistance) isomer and vice versa.

4. Discussion

Our principal result is a direct measurement of the resistance of the two isomers of the photochrome when they are part of the break junction circuit, namely 526±90 MΩ in the open form **1o** and 4±1 MΩ in the closed form **1c**. Importantly, our results are in quite good agreement with the results of the first-principles simulations we report here. The use of theoretical results for a gold on-top site seems the most reasonable, given that the molecule is attached to a stretched gold nanofilament [22]. These results add another molecule to the list for which single-molecule data are in reasonable agreement with first principles calculations [12], suggesting that the very large discrepancies in earlier work [38] are the result of uncertainties about the bonding arrangements and number of molecules in the measurement device.

Dulic *et al.* [5] have recently reported measurements on a related dithienylethene molecule, differing in that the rings attached to the central portion of the molecule were thiophenes (as opposed to the phenyl rings used here). They did not report quantitative data for resistance values, but indicate in their paper that the open form had a resistance 'in the GΩ range' while the closed molecules had a resistance in the 'MΩ' range. Within these limits, the results of the two sets of measurements are in general agreement. Dulic *et al.* [5] report a ratio of open to closed resistance of 1000 to 1, about an order of magnitude higher than our value of 131. The differences between the results of the two studies likely reflect in part differences in molecular structure.

Differences between the two studies also arise in the switching behavior observed on metal surfaces. Dulic *et al.* report that the molecule can be switched on metal surfaces from the closed to the open form using VIS exposure. This was found to be the case both

for molecules in a junction, and for molecules attached to gold nanoparticles in solution (where the isomer ratio was determined by absorption spectroscopy). They found that the molecules they studied could not be switched from the open to the closed form, even upon extended irradiation with UV light. In contrast, our spectroscopic measurements on thin gold films indicate repeated, reversible switching in both directions for **1** and **2**. We found this to be the case both with the gold films described here, and with molecules attached to gold nanoparticles in solution (the approach used by Dulic *et al*.) although those data are not shown because of the possibility that molecules could desorb, photoisomerize in solution, and reattach. This possibility is eliminated in the approach we report here. Another difference lies with the wavelength used for irradiation of the open form. Dulic *et al.* used 313 nm, a wavelength that resulted in photodamage when we employed it with our samples (as evidenced by non-reversible changes in the switching behavior).

We observed photoisomerization in both directions for molecules on the surfaces of thin gold layers and on the thicker substrates used for break junctions, although the apparent quantum yields of the UV-induced isomerizations were lower under these conditions than they are in solution. The break junction measurements in particular suggest inefficient photoisomerization to the closed isomer. This trend is consistent with the results of Dulic, *et al.*, who observed no such isomerization. Presumably, the decreased quantum yields of photoisomerization of molecules on gold are due to a shortening of the lifetime of the photochrome excited state due to interactions with the metal plasmon.

We noted that the apparent quantum yield of photoisomerization under UV irradiation was lower on the surface used for the break junctions (as determined by conductance measurements) than it was for molecules attached to thin gold layers (as determined by UV-VIS absorption measurements). One possible reason for this could be a difference in gold structure. This seems to us to be an unlikely explanation. AFM images of the thin gold films show that the gold forms as isolated clusters of 50-100 nm in diameter, big enough to behave like the bulk gold in the break junction experiments [39]. Another possibility is that the break junction measurements do not sample the population of isomers on the gold surface ideally. This could occur if the closed isomers **1c** do not span the junctions as readily as the open isomers **1o**. Such a situation would lead to the apparently reduced yield of closing seen in Figure 7b. The results from the fixed gap measurements are consistent with this possibility. Far fewer "well behaved" gaps containing molecules were found for the closed form of the photochrome than for the open form

In all of our studies, we noted that data appeared to be "noisy" at high bias. We believe that the appearance of this noise is not completely random. It is interesting to note that the voltage range over which data can be obtained correlates with the HOMO-LUMO gap of the molecules (see Figure 5). He *et al.* [40] have shown that changes in the redox state of nanoscale polymer wires occur as 'telegraph noise', presumably reflecting switching in the environmental polarization state owing to the atomic scale of the measurement. Thus noise might well be an indicator of the onset of redox activity at the nanoscale, and therefore its onset would correlate with the HOMO-LUMO gap.

5. Conclusions

In conclusion, we have shown that the electrical properties of two forms of a photochromic molecule can be measured quite accurately by the method of repeated break junction formation recently introduced by Xu and Tao [11]. The values for the single molecule resistance for the two forms obtained in this way are in reasonable agreement with first-principles simulations (within a factor two). The ratio of open to closed resistance is in good agreement with theory. We find that in spite of presumed quenching of photochrome excited states by the gold plasmon, photoisomerization in both directions is observed on the gold surfaces. The apparent quantum yield of UV-induced isomerization of **1o** to **1c** under break junction conditions tends to be lower than for isomerization on thin evaporated gold films. Thus, while the switching properties of the molecule are profoundly affected by the metal surface, the molecules still retain their function. This indicates that there are possibilities for fabricating opto-electronic devices from molecules attached to electrode surfaces.

Acknowledgment

This work was supported by grants from the National Science Foundation (ECS-01101175 and CHE-0352599). JA is grateful to the Carl Trygger Foundation for Scientific Research for a grant in support of postdoctoral research.

Table 1. Examples of current peak values (I_m) in the current histograms for **1o** and **1c**.

Bias (V)	Peak 1		Peak 2		Peak 3	
			Open Isomer (**1o**)			
	$(I_m)1$ (nA)	$(I_m)1/(I_m)1$	$(I_m)2$ (nA)	$(I_m)2/(I_m)1$	$(I_m)3$ (nA)	$(I_m)3/(I_m)1$
0.10	0.19±0.1	1.00	0.39±0.2	2.05	0.60±0.3	3.15
0.15	0.27±0.1	1.00	0.58±0.3	2.14	0.89±0.4	3.29
0.20	0.37±0.1	1.00	0.78±0.3	---	NA	---
			Closed Isomer (**1c**)			
0.08	20±3	1.0	39±8	1.95	63±20	3.15
0.10	25±2.5	1.0	50±10	2.00	74±15	2.96
0.12	30±3	1.0	61±12	2.03	NA	---

[a] The errors are the approximate half-widths at half height of the peaks.

References

[1] Chance R R, Prock A and Silbey R 1978 *Adv. in Chemical Physics* **37** 1

[2] Yang T J, Lessard G A and Quake S R 2000 *App. Phys. Lett.* **76** 378

[3] Imahori H, Norieda H, Nishimura Y, Yamakazi I, Higuchi K, Kato N, Motohiro T, Yamada H, Tamaki K, Arimura M and Sakata Y 2000 *J. Phys. Chem B* **104** 1253

[4] Doron A, Katz E, Tao G and Willner I 1997 *Langmuir* **13** 1783

[5] Dulic C, van der Molen S J, Kudernak T, Jonkman H T, De Jong J J D, Bowden T N, van Esch J, Feringa B L and van Wees B J 2003 *Phys. Rev. Lett.* **91** 207402-207402-2

[6] Reed M A, Zhou C, Muller C J, Burgin T P and Tour J M 1997 *Science* **278** 252

[7] Reichert J, Ochs R, Beckmann D, Weber H B, Mayor M and von Lohneysen H 2002 *Phys. Rev. Lett.* **88** 176804

[8] Collier C J, Wong E W, Belohradsky M, Raymo F M, Stoddart J F, Kuekes P J, Williams R S and Heath J R 1999 *Science* **285** 391

[9] Kushmerick J G, Holt D B, Yang J C, Naciri J, Moore M H and Shashidhar R 2002 *Phys. Rev. Lett.* **89** 086802-086802-4

[10] Cui X D, Primak A, Zarate X, Tomfohr J, Sankey O F, Moore A L, Moore T A, Gust D, Harris G and Lindsay S M 2001 *Science* **294** 571

[11] Xu B and Tao N J 2003 *Science* **301** 1221

[12] Tomfohr J K and Sankey O F 2004 *J. Chem. Phys.* **120** 15542

[13] Eckert J F, Nicoud J F, Nierengarten J F, Liu S G, Echegoyen L, Barigelletti F, Armaroli N, Quali L, Krasnikov V and Hadziioannou G 2000 *J. Am. Chem. Soc.* **122** 7467

[14] Sylvain L, Kawai S H and Lehn M J 1995 *Chem. Eur. J.* 275

[15] Dudek S P, Sikes H D and Chidsey C E D 2001 *J. Am. Chem. Soc.* **123** 8033

[16] DeRose J A, Lampner D B and Lindsay S M 1993 *J. Vac. Sci. Technol.* **A11** 776

[17] Leatherman G, Durantini E N, Gust D, Moore T A, Moore A L, Stone S, Zhou Z, Rez P, Liu Y Z and Lindsay S M 1999 *J. Phys. Chem. B* **103** 4006

[18] Li C Z, He X E and Tao N J 2000 *Appl. Phys. Lett.* **77** 3995

[19] Park H, Lim A K L, Alivisatos A P, Park J and McEuen P L 1999 *Appl. Phys. Lett.* **74** 301

[20] Dulkeith E, Morteani T, Klar T A, Feldmann J, Levi S A, van Veggel F C J M, Reinhoudt D N, Moller M and Gittins D I 2002 *Phys. Rev. Lett.* **89** 203002

[21] Wanunu M, Vaskevich A and Rubinstein I 2004 *J. Am. Chem. Soc.* **126** 5569

[22] Xu B, Xiao X and Tao N J 2003 *J. Am. Chem. Soc.* **125** 16164

[23] Landauer R 1989 *J. Phys. Condens. Matter* **1** 8099

[24] Büttiker, Imry Y, Landauer R and Pinhas S 1985 *Phys. Rev.* **B31** 6207

[25] Mujica V, Kemp M and Ratner M A 1994 *J. Chem. Phys.* **101** 6849

[26] Datta S 1990 *Electronic transport in mesoscopic systems* Cambridge (Cambridge University Press)

[27] Tomfohr J and Sankey O F 2002 *Phys. Rev. B* **65** 245105

[28] Lewis J P, Glaesemann K R, Voth P, Fritsch J, Demkov A A, Ortega J and Sankey O F 2001 *Phys. Rev. B* **64** 195103

[29] Demkov A A, Ortega J, Sankey O F and Grumbach M P 1995 *Phys. Rev.* **B52** 1618

[30] Sankey O F and Niklewski D J 1989 *Phys. Rev. B* **40** 3979

[31] Li J, Tomfohr J K and Sankey O F 2003 *Physica E: Low-dimensional Systems and Nanostructures* **19** 133

[32] Suhai S 1995 *Phys. Rev. B* **51** 16553

[33] Schmidt M W, Baldridge K K, Boatz J A, Elbert S T, Gordon M S, Jensen J J, Koseki S, Matsunaga M, Nguyen K A, Su S, Windus T L, Dupuis M and Montgomery J A 1993 *J. Comput. Chem.* **14** 1347

[34] Kondoh H, Iwasaki M, Shimada T, Amemiya K, Yokoyama T, Ohta T, Shimomura T and Kono S 2003 *Phys. Rev. Lett.* **90** 066102-066102-4

[35] Sellers H, Ulman A, Shnidman Y and Eilers J E 1993 *J. Am. Chem. Soc.* **115** 9389

[36] Ramachandran G K, Tomfohr J, Li J, Sankey O F, Zarate X, Primak A, Terazono Y, Moore T A, Moore A L, Gust D, Nagahara L A and Lindsay S M 2003 *J. Phys. Chem B* **107** 6162

[37] Lee T H and Dickson R M 2003 *J. Phys. Chem. B.* **107** 7387

[38] Salomon A, Cahen D, Lindsay S, Tomfohr J, Engelkes V B and Frisbie C D 2003 *Advanced Materials* **15** 1881

[39] Wang B, Wang H, Li H, Zeng C and Hou J G 2000 *Phys. Rev. B* **63** 035403-035403-7

[40] He H X, Li X L, Tao N J, Nagahara L A, Amlani I and Tsui R 2003 *Phys. Rev. B* **68** 045302

Figure Captions

Figure 1: Structure and photoisomerization reactions of dithienylethene photochromes **1** and **2**, and the synthetic scheme for their preparation. Open (left) and closed (right) isomers are shown at the top.

Figure 2: Schematic representations of the two types of conductance measurements used in this work. (a) Break junction formed by pushing a gold probe tip into a gold surface covered with dithiolated dithienylethene molecules, retracting it and recording current as molecules become transiently trapped in the gap. (b) Nanostructured gold electrodes on native silicon oxide with trapped molecules spanning a gap fabricated by electromigration. The gap is exposed through a window in an insulating layer of silicon nitride. (c) An SEM image of a 60 nm wide EBL fabricated wire broken by electromigration at the point marked by the arrow.

Figure 3: (a) STM images of a clean Au(111) substrate , (b) a substrate covered with dithiolated molecules in the closed form (**1c** in Figure 1), and (c) in the open form (**1o** in Figure 1). Images were made with a gold probe in toluene with a tunnel current of 10 pA and a tip bias of -1.0 V. The corresponding current-distance traces for break junction measurements are shown below: (d) Clean surfaces show rapid decay of current with no steps. (e) The closed molecules give rise to steps at about 4 MΩ (and/or submultiples thereof). (f) The open molecule gives rise to steps at about 500 MΩ; in this case the curves show evidence of switching between 500 MΩ (1 molecule) and 250 MΩ (2 molecules).

Figure 4: Current histograms built from current-distance traces (c.f. Figure 3) for (a) open molecules **1o** and (b) closed molecules **1c** at various biases as marked. Gaussian fits to each peak in the series (N=1, 2... molecules) are shown as white lines.

Figure 5: Current-voltage data (open circles) for (a) open molecules **1o** and (b) closed molecules **1c** (error bars are ± HWHM of the Gaussian fits shown in Figure 4). Calculated current-voltage curves for molecules attached to hollow sites (triangles) and on-top sites (squares) are also shown.

Figure 6: Conversion of isomers **1o** and **1c** on a thin gold surface in an argon atmosphere as determined by UV-VIS absorption spectroscopy. (a) Difference absorption spectra (spectrum minus initial spectrum of **1o**) as a function of exposure of films of initially open molecules to UV at 366 nm. The solid lines are, in order of *increasing* ΔA at 650 nm, spectra obtained after 1, 6, 11, 16, and 21 min of UV irradiation. The growth of the band at 650 nm indicates conversion of **1o** to the closed form **1c**. (b) The solid lines are, in order of *decreasing* ΔA at 650 nm, spectra obtained from the same sample (following UV irradiation as in part (a)) after 0, 30, 90, 170, 230, and 290 min of irradiation with red light (~590-900 nm) as described in the text. The band at 650 nm disappears as the molecules convert back to the open form. Subsequent to the final exposure with red light, a second exposure to UV light isomerizes the molecules to the closed form once again, as indicated by the dotted line in part (a).

Figure 7: Electrical measurement of optical switching on Au in the break junction experiment. (a) After application of a solution of closed molecules **1c** to the gold surface followed by rinsing to remove unbound material, 70% of the measurements gave resistances characteristic of the closed form with a minority (30%) in the open form (bar set I). After exposure to 643 nm light, the population is evenly split between open and closed forms (bar set II). Subsequent exposure of this surface to 366 nm radiation increases the fraction of closed molecules (bar set III). (b) After application of a solution of open molecules **1o** to the gold surface followed by rinsing to remove unbound material, 67% of the measurements gave resistances characteristic of the open form and 33% gave results representing the closed form (bar set I). Subsequent exposure of this surface to 643 nm light increases the fraction of closed molecules slightly (bar set II).

Figure 8: Distribution of measured resistances for photochromic molecules **1** inserted into nanofabricated junctions for (a) the closed form **1c** and (b) the open form **1o**. Points are the fraction of the total number of 'successful' junctions that give resistances lying in a particular decade (10^4 to 10^5 Ω is shown by the point at 10^5 Ω and so on). Arrows mark the expected resistances based on the break junction measurements.

Figure 1

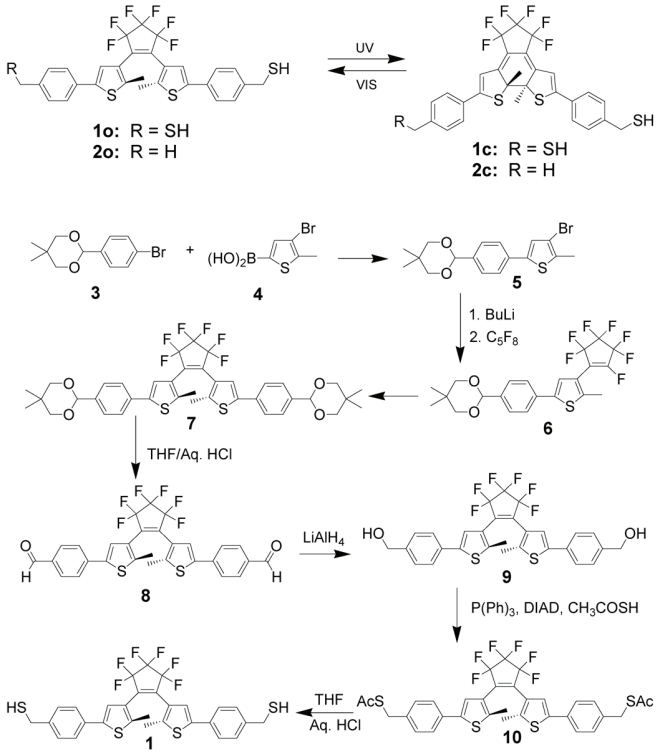
UV
VIS
1o: R = SH
2o: R = H
1c: R = SH
2c: R = H
3
4
5
1. BuLi
2. C5F8
6
7
THF/Aq. HCl
8
LiAlH4
9
P(Ph)3, DIAD, CH3COSH
10
THF
Aq. HCl
1

Figure 2

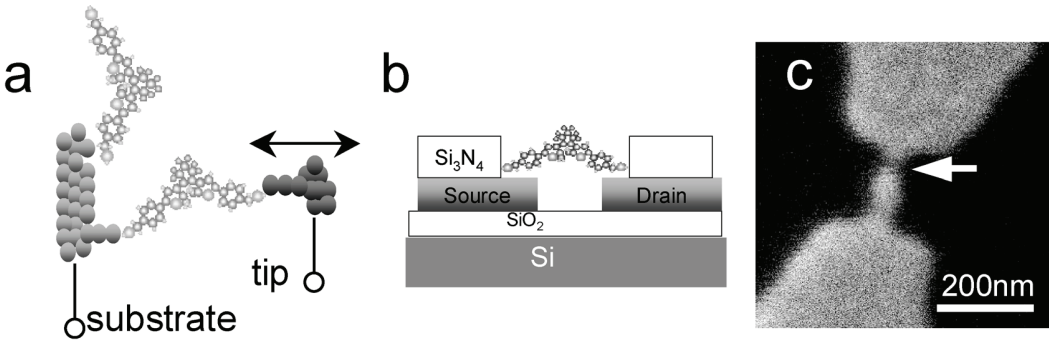

Figure 3

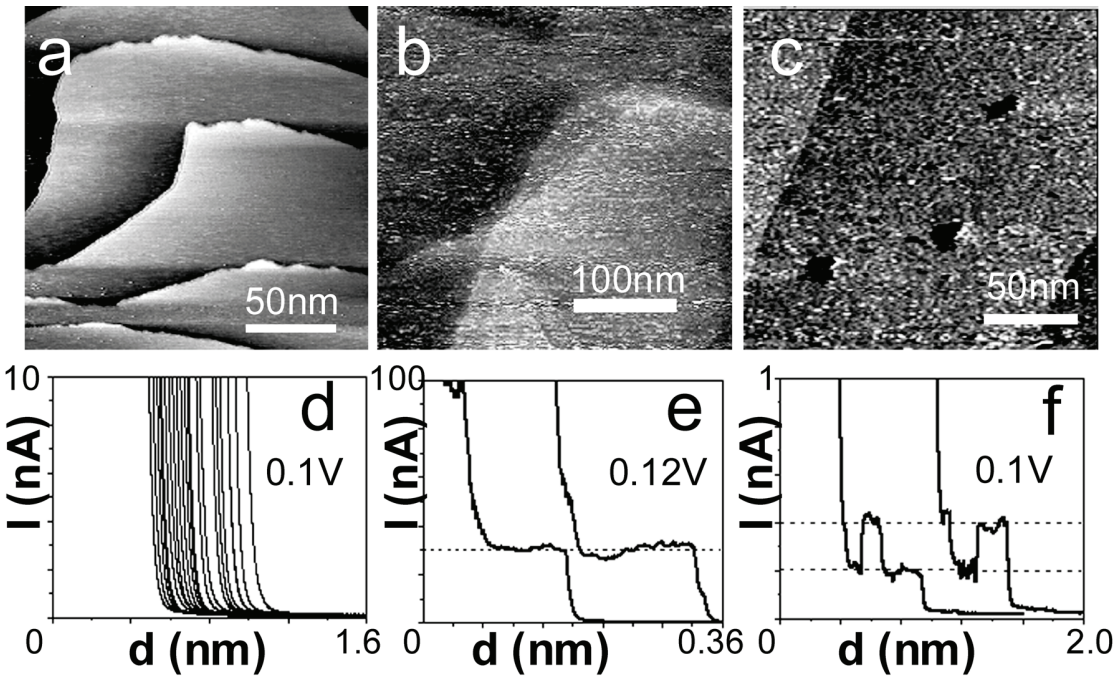
a
50nm
b
100nm
c
50nm
10
I (nA)
d
0.1V
0
d (nm)
1.6
100
I (nA)
e
0.12V
0
d (nm)
0.36
1
I (nA)
f
0.1V
0
d (nm)
2.0

Figure 4

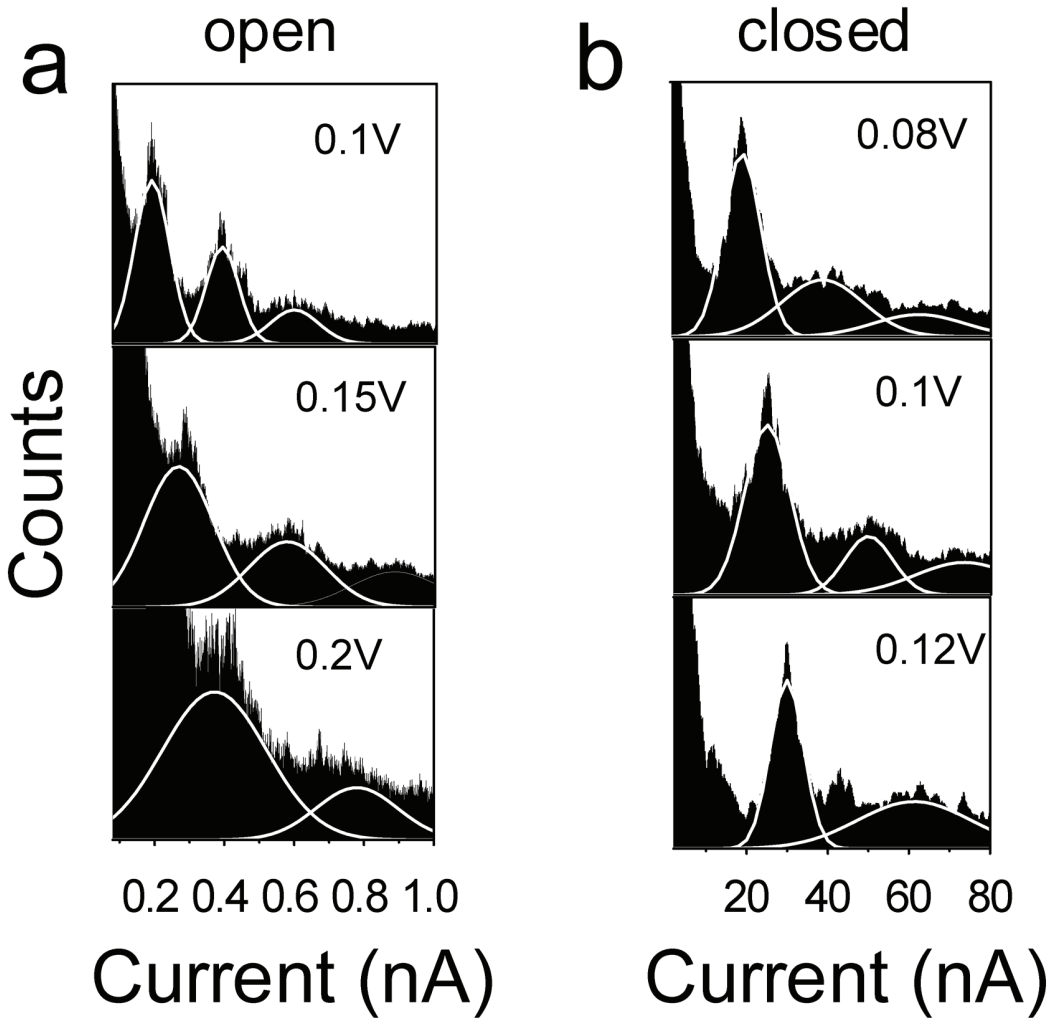
a
open
b
closed
0.1V
0.15V
0.2V
0.08V
0.1V
0.12V
Counts
0.2 0.4 0.6 0.8 1.0
20 40 60 80
Current (nA)
Current (nA)

Figure 5

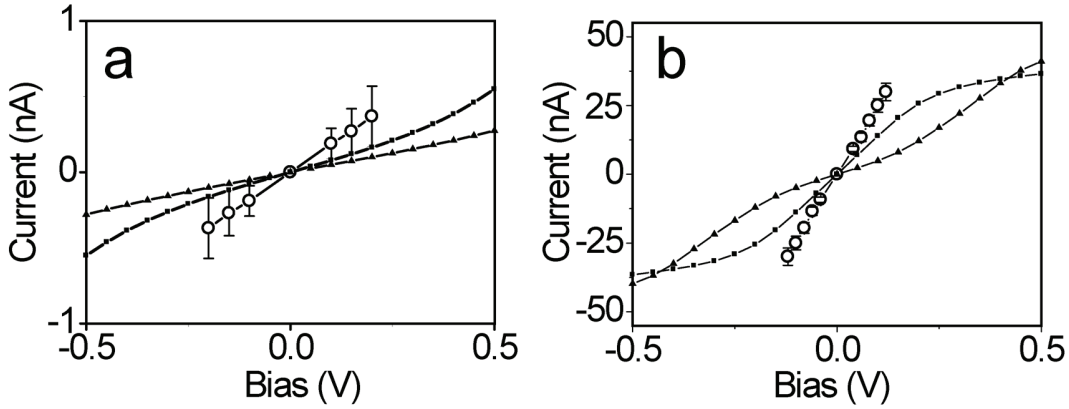

Figure 6

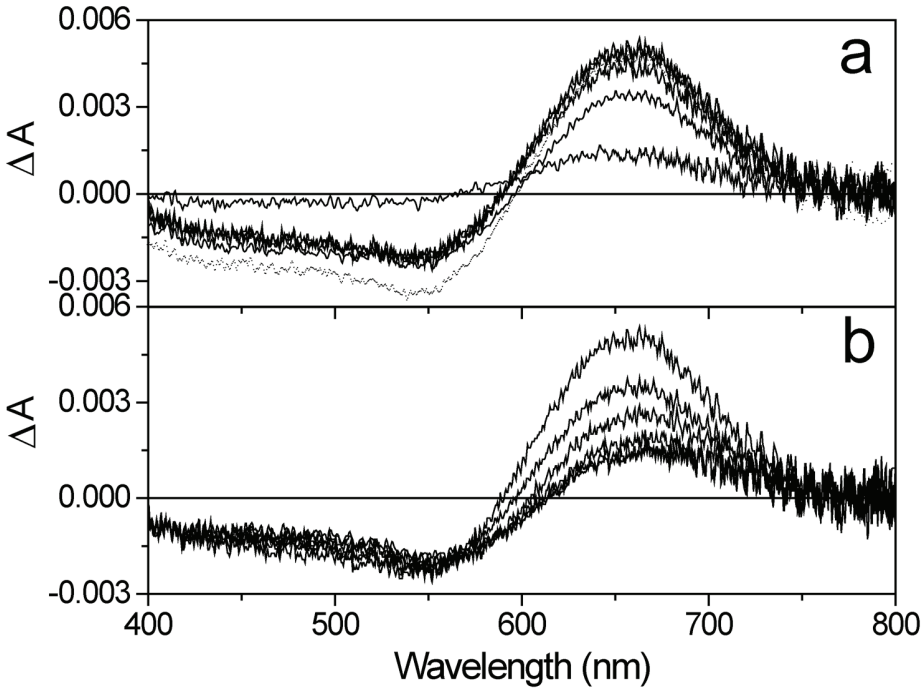
0.006
0.003
0.000
-0.003
ΔA
a
0.006
0.003
0.000
-0.003
ΔA
b
400
500
600
700
800
Wavelength (nm)

Figure 7

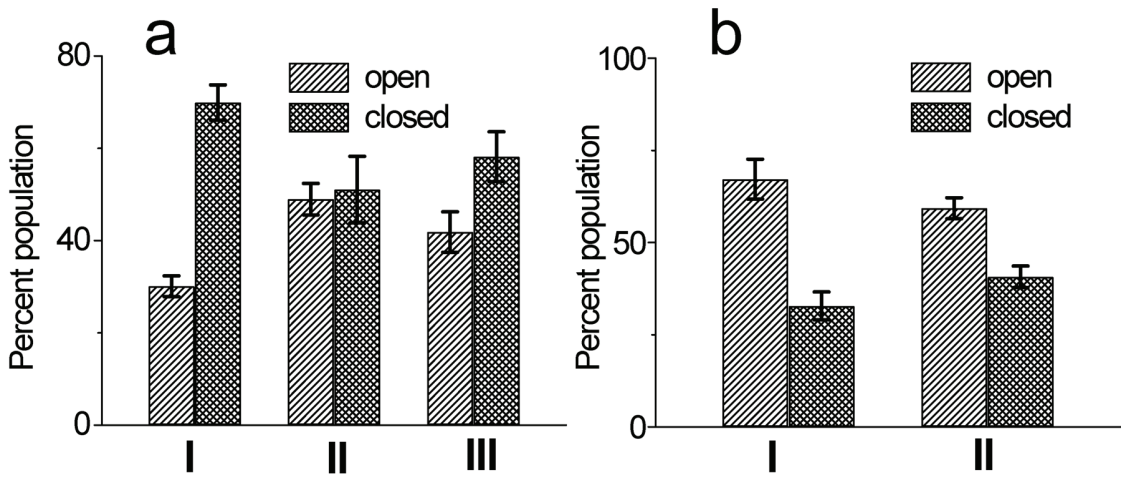
a
80
40
0
Percent population
open
closed
I
II
III
b
100
50
0
Percent population
open
closed
I
II

Figure 8

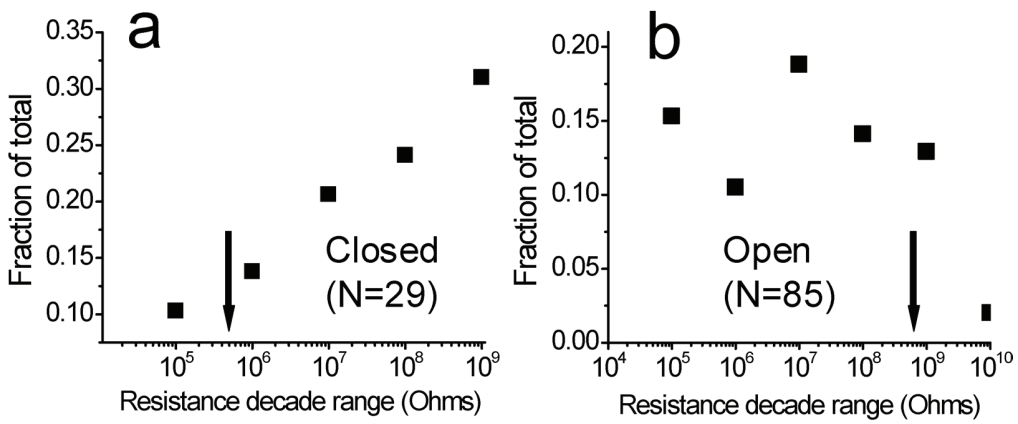
a
Fraction of total
0.35
0.30
0.25
0.20
0.15
0.10
Closed
(N=29)
10^5 10^6 10^7 10^8 10^9
Resistance decade range (Ohms)
b
Fraction of total
0.20
0.15
0.10
0.05
0.00
Open
(N=85)
10^4 10^5 10^6 10^7 10^8 10^9 10^{10}
Resistance decade range (Ohms)